

Vibration of Thin Beams by PIM and RPIM methods

*B. Kanber¹, and O. M. Tufik¹

¹Mechanical Engineering Department, University of Gaziantep, Turkey.

*Corresponding author: kanber@gantep.edu.tr

Abstract

In this study, vibration of thin beams are analyzed by using point interpolation (PIM) and radial point interpolation (RPIM) methods with standard Gaussian integration and a nodal integration based on the Taylor series expansion. The effects of integration schemes, support domain sizes and RPIM shape parameters on the vibration modes are investigated. A cantilever beam problem is solved by linear elastic materials with uniform cross-section. The results are compared with finite element and available analytical solutions.

Keywords: PIM, RPIM, Vibration, Meshfree, Thin Beams.

Introduction

The PIM (Liu and Gu, 2001a) and RPIM (Wang and Liu, 2002a, 2002b) are meshfree techniques that are used in the solution of wide range of engineering problems. In addition to these applications, their local versions are used to analyze the vibration of thin beams and 2-D solids (Liu and Gu, 2001b; Gu and Liu, 2000).

In this study, PIM and RPIM solutions of vibration of thin beams are carried out using the standard Gauss integration scheme and a nodal integration scheme based on Taylor Series expansion. The effect of support domain sizes and shape parameters of RPIM are investigated on the natural frequencies and free vibration modes.

Free Vibrations of Thin Beams

The Lagrangian can be written as follows (Chandrupatla and Belegundu, 1999):

$$L = T - \Pi \quad (1)$$

where T is the kinetic energy and Π is the potential energy of the beam. Using Eq. (1), Hamilton's principle can be expressed as:

$$\int_{t_1}^{t_2} \delta L = 0 \quad (2)$$

Then, for the free vibration, the equation of motion can be obtained using Eq. 2 as follows:

$$\mathbf{M}\ddot{\mathbf{Q}} + \mathbf{K}\mathbf{Q} = 0 \quad (3)$$

where \mathbf{Q} is the global displacement vector, \mathbf{M} is the global mass matrix and \mathbf{K} is the global stiffness matrix. For the steady state condition, starting from equilibrium state, we set:

$$\mathbf{Q} = \mathbf{U}\sin(\omega t) \quad (4)$$

where \mathbf{U} is the vector of nodal amplitudes of vibration and ω is the circular frequency. Introducing Eq. (4) into Eq. (3), we have:

$$\mathbf{K}\mathbf{U} = \omega^2\mathbf{M}\mathbf{U} \quad (5)$$

where \mathbf{U} corresponds to the eigenvalue, $\lambda = \omega^2$.

The global mass and stiffness matrixes can be obtained assembling their nodal values as in the FEM. Their nodal values are,

$$\mathbf{k} = E I \int_{x_1}^{x_2} \mathbf{N}^T \mathbf{N} dx \quad (6)$$

$$\mathbf{m} = \rho A \int_{x_1}^{x_2} \mathbf{N}^T \mathbf{N} dx \quad (7)$$

where E is the modulus of elasticity, I is the second moment of area, ρ is the material density and A is the cross-sectional area of the beam. They are assumed constant through an integration cell. x_1 and x_2 are the limits of an integration cell. \mathbf{N} is the shape function vector that can be replaced with either PIM or RPIM shape functions. They are calculated in terms of real coordinates. So, they must be transformed to natural coordinates of -1 and 1 for Gauss integration scheme. It is not required to transform the limits to the natural limits when the nodal integration scheme is used.

Point Interpolation Method (PIM)

In the thin beam theory, there are two degrees of freedom at each node: deflection and slope. Therefore, $u(x)$ at the point of interest x_Q is approximated by $2n$ terms as presented by Liu (2010):

$$u(x, x_Q) = \sum_{i=1}^{2n} B_i(x) a_i \quad (8)$$

where $B_i(x)$ is the basis function defined in the Cartesian coordinate, a_i is the coefficient for the basis function, n is the number of nodes in a local support domain.

When, the polynomial basis function is used as a basis function Eq. (8) can be written as:

$$u(x, x_Q) = \sum_{i=1}^{2n} p_i(x) a_i(x_Q) = \mathbf{p}^T(x) \mathbf{a}(x_Q) \quad (9)$$

where $p_i(x)$ is the basis function of monomials, a is the coefficient of basis function $p_i(x)$. A polynomial basis in one dimension is:

$$\mathbf{p}^T(x) = [1, x, x^2, x^3, \dots, x^{2n-1}] \quad (10)$$

At node i , we have equation in matrix form as:

$$u^{sd} = \mathbf{P}_Q \mathbf{a} \quad (11)$$

where generalized displacement vector \mathbf{u}^{sd} :

$$\mathbf{u}^{sd} = \{[w_1, \theta_1, w_2, \theta_2, \dots, w_n, \theta_n]^T\} \quad (12)$$

and \mathbf{P}_Q is the moment matrix. For 1D case, it is given by:

$$\mathbf{P}_Q = [\mathbf{p}(x_1), \mathbf{p}(x_2), \dots, \mathbf{p}(x_{2n})]^T \quad (13)$$

If the inverse of moment matrix exists, using Eq. (11), we have:

$$\mathbf{a} = \mathbf{P}_Q^{-1} \mathbf{u}^{sd} \quad (14)$$

Finally, the Eq. (9) becomes:

$$u(x, x_Q) = \sum_{i=1}^n p_i(x) a_i(x_Q) = \mathbf{p}^T \mathbf{P}_Q^{-1} \mathbf{u}^{sd} \quad (15)$$

where PIM shape function ϕ :

$$\phi = \mathbf{p}^T \mathbf{P}_Q^{-1} = [\phi_1(x) \quad \phi_2(x) \quad \dots \quad \phi_n(x)] \quad (16)$$

Radial Point Interpolation Method (RPIM)

Radial basis functions are used in PIM to create shape functions. The field variable is approximated using a radial basis function by considering deflection and slope at each node. Thus, equation Eq. (8) becomes:

$$u(x, x_Q) = \sum_{i=1}^{2n} B_i(x) a_i = \mathbf{R}^T(x) \mathbf{a}(x_Q) \quad (17)$$

where \mathbf{a} is the unknown constants vector for the radial basis function, \mathbf{R} is the radial basis function with distance r between points x and x_i . For 1D case, r can be written as:

$$r = x - x_i \quad (18)$$

As a vector form, \mathbf{R} :

$$\mathbf{R}^T = [R_1(r_1)^0, R_2(r_2)^1, R_3(r_3)^2, \dots, R_n(r_n)^{2n-1}] \quad (19)$$

In this study, multiquadric radial basis function (MQ RBF) $((r_i^2 + (\alpha_c * d_c)^2)^q)$ is used to construct shape functions. In general form of MQ RBF, it has two shape parameters, α_c and q , which control the shape of functions and their range of values are proposed by Wang and Liu (2002). d_c is the nodal spacing in whole problem domain. If the nodes are uniformly distributed, it is equal to the distance between two nodes. Else, it is equal to the average nodal spacing. These parameters can be altered to increase the solution accuracy for different type of problems.

The coefficients a_i in Eq. (17) can be determined by letting Eq. (17) be satisfied at all the n support nodes as given by Liu (2010). After interpolation at k th point, we have:

$$u_k = u(x_k) = \sum_{i=1}^{2n} a_i R_i(x_k) \quad k = 1, 2, \dots, n \quad (20)$$

The equation above can be written in matrix form as:

$$u^{sd} = \mathbf{R}_Q \mathbf{a} \quad (21)$$

where u^{sd} is the generalized displacement vector, and \mathbf{R}_Q is the moment matrix of RBFs:

$$\mathbf{R}_Q = \begin{bmatrix} R_1(r_1)^0 & R_2(r_1)^1 & \dots & R_n(r_1)^{2n-1} \\ R_1(r_2)^0 & R_2(r_2)^1 & \dots & R_n(r_2)^{2n-1} \\ \vdots & \vdots & \ddots & \vdots \\ R_1(r_n)^0 & R_2(r_n)^1 & \dots & R_n(r_n)^{2n-1} \end{bmatrix} \quad (22)$$

It is the invertible moment matrix and vector of coefficients \mathbf{a} can be calculated as:

$$\mathbf{a} = \mathbf{R}_Q^{-1} u^{sd} \quad (23)$$

Substituting Eq. (23) into Eq. (17):

$$u(x, x_Q) = \mathbf{R}^T(x) \mathbf{R}_Q^{-1} u^{sd} \quad (24)$$

where RPIM shape functions $\phi(x)$ are:

$$\phi(x) = \mathbf{R}^T(x) \mathbf{R}_Q^{-1} = [\phi_1(x) \ \phi_2(x) \ \dots \ \phi_n(x)] \quad (25)$$

Integration Schemes

Gauss Integration Scheme

To evaluate Eqs. (6) and (7), two different integration schemes are used. The first one is standard Gauss integration. In this method, quadrature cells (background cells) are used to integration. The shape functions are calculated for each node in the support domain.

Two sampling points are used to calculate flexural nodal stiffness matrix and one sampling point is used for shear nodal stiffness matrix calculation. Thus,

$$\mathbf{k} = E I \text{Jac} [w_1(\mathbf{N}_{q1}^T \mathbf{N}_{q1}) + w_2(\mathbf{N}_{q2}^T \mathbf{N}_{q2})] \quad (26)$$

$$\mathbf{m} = \rho A \text{Jac} [w(\mathbf{N}_q^T \mathbf{N}_q)] \quad (27)$$

where Jac is the Jacobian matrix, w , w_1 , w_2 are weights, q , q_1 , q_2 are quadrature points.

Nodal Integration Scheme

Second integration scheme is the nodal integration proposed by Liu et al. (2007). In this method, nodal stiffness matrices are introduced by Taylor's expansion. The whole solution domain is divided into non-overlapping cells around each field node (Fig. 1). Thus, the nodal stiffness matrices can be expressed as:

$$\mathbf{k} = E I \left\{ \begin{aligned} &(\mathbf{N}_{x_0}^T \mathbf{N}_{x_0})(d_{x2} - d_{x1}) + \frac{1}{2!} \cdot \frac{\partial}{\partial x} (\mathbf{N}_{x_0}^T \mathbf{N}_{x_0})(d_{x2}^2 - d_{x1}^2) \\ &+ \frac{1}{3!} \frac{\partial^2}{\partial x^2} (\mathbf{N}_{x_0}^T \mathbf{N}_{x_0})(d_{x2}^3 - d_{x1}^3) \end{aligned} \right\} \quad (28)$$

$$\mathbf{m} = \rho A \left\{ \begin{aligned} &(\mathbf{N}_{x_0}^T \mathbf{N}_{x_0})(d_{x2} - d_{x1}) + \frac{1}{2!} \cdot \frac{\partial}{\partial x} (\mathbf{N}_{x_0}^T \mathbf{N}_{x_0})(d_{x2}^2 - d_{x1}^2) \\ &+ \frac{1}{3!} \frac{\partial^2}{\partial x^2} (\mathbf{N}_{x_0}^T \mathbf{N}_{x_0})(d_{x2}^3 - d_{x1}^3) \end{aligned} \right\} \quad (29)$$

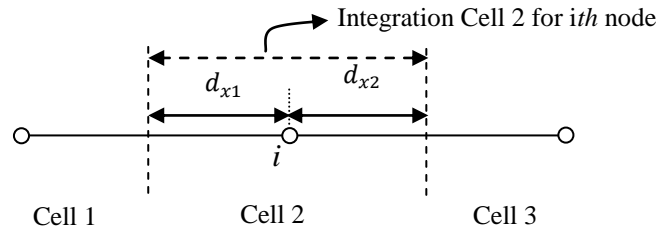


Figure.1 Nodal integration scheme

Solutions and Discussions

A cantilever beam of uniform rectangular cross section ($0.1 \times 0.01 \text{ m}^2$) is used to test the developed programs as shown in Fig. 2. Structural steel is used with a Young's modulus of 200 GPa and density of 7840 kg/m^3 . 1 kN end load is applied. 100 two-node finite elements are used in the FEM solutions. 11 regular distributed nodes are used in the PIM and RPIM solutions. The codes are developed in Matlab and the function "eig" is used to find eigenvalues and eigenvectors. All methods are in excellent agreements with analytical and finite element solutions as shown in Fig. 3 for the vertical deflection of the cantilever beam.

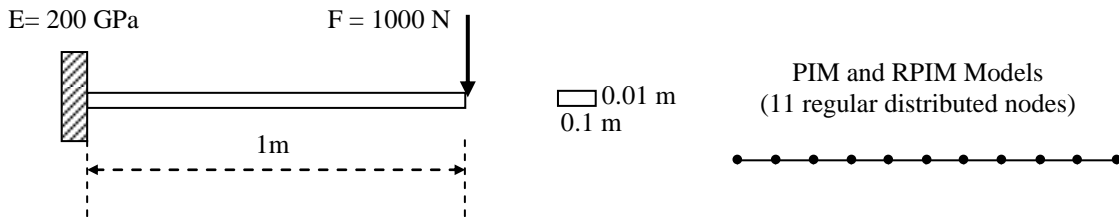


Figure 2. Cantilever beam and its PIM and RPIM models.

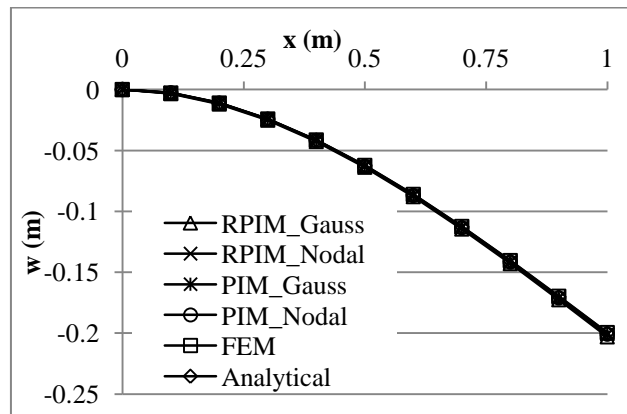
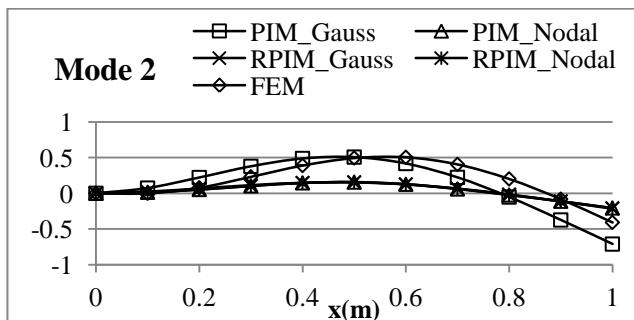
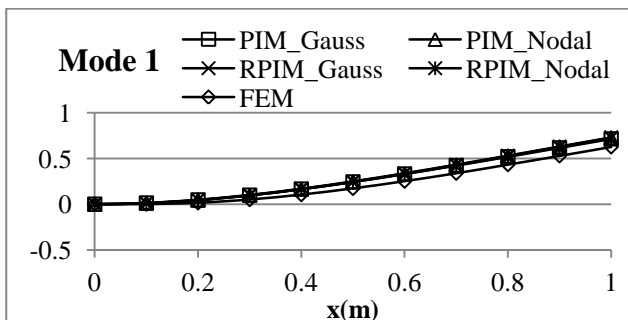


Figure 3. Vertical deflections of the cantilever beam under 1kN end load ($ds=3L/2$ for PIM and RPIM, $q=1$, $\alpha_c=3$ for RPIM).

First four modes of vibration of cantilever beam are given in Fig. 4. In these solutions, support domain size is used as $3L/10$ for PIM and RPIM. q and α_c are used as 1 and 3 respectively for the RPIM. In the first mode, all methods are in good agreements with the FEM solution. However, when the mode number is increased, PIM and RPIM with nodal integration and RPIM with Gauss integration give more stiff results than others.



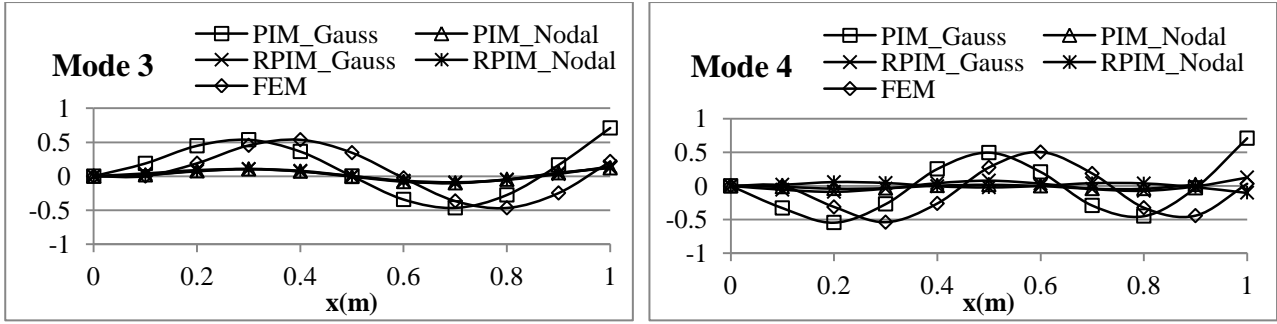


Figure 4. First four free vibration modes of the cantilever beam ($ds=3L/10$ for PIM and RPIM, $q=1$, $\alpha_c=3$ for RPIM).

The PIM and RPIM values of frequencies are compared with FEM and exact solutions in Table 1-4 for standard Gauss and nodal integration schemes, for different support domain sizes and shape parameters. Increasing the support domain size (sd) up to $5L/10$ slightly change the PIM frequencies when the standard Gauss integration scheme is used as shown in Table 1. However, when sd becomes equal to $5L/10$, frequencies suddenly drops. When the nodal integration scheme (based on Taylor series expansion) is used, the PIM frequencies in the first mode are slightly improved, but the frequencies in the higher modes get worse. Similar results are also obtained for RPIM frequencies as shown in the Table 2. The best results are obtained when the support domain size is equal to $L/10$ with Gauss and nodal integration schemes. The change of α_c and q values does not significantly change the frequencies as shown in the Table 3 and 4. Although q causes singular moment matrix problem when it is equal to 1 (Liu and Gu, 2005), it does not cause a singularity problem in this study.

Table 1. PIM frequencies of the cantilever beam for various support domain (sd) sizes.

Mode	PIM with Gauss integration (11 nodes)					PIM with Nodal integration (11 nodes)					FEM (100 elements)	Exact (Ferreira, 2009)
	sd					sd						
	L/10	2L/10	3L/10	4L/10	5L/10	L/10	2L/10	3L/10	4L/10	5L/10		
1	3.516	3.516	3.503	3.042	1.117	3.490	3.497	3.501	3.500	3.448	3.516	3.516
2	22.035	22.026	21.870	18.502	12.096	20.183	21.000	22.273	21.623	20.471	22.034	22.035
3	61.707	61.646	60.855	50.439	38.793	38.448	5.560	39.697	57.500	66.965	61.697	-
4	120.966	120.719	117.678	97.908	87.656	45.109	39.276	53.846	39.200	39.713	120.902	-

Table 2. RPIM frequencies of the cantilever beam for various support domain (sd) sizes ($\alpha_c=3$, $q=1$).

Mode	RPIM with Gauss integration (11 nodes)					RPIM with Nodal integration (11 nodes)					FEM (100 elements)	Exact (Ferreira, 2009)
	sd					sd						
	L/10	2L/10	3L/10	4L/10	5L/10	L/10	2L/10	3L/10	4L/10	5L/10		
1	3.515	3.512	3.486	2.809	0.944	3.523	3.505	3.502	3.499	3.425	3.516	3.516
2	22.035	21.953	21.626	17.505	13.887	20.471	20.724	22.311	21.097	20.424	22.034	22.035
3	61.656	61.398	59.818	47.277	26.530	39.107	39.353	39.906	39.399	39.614	61.697	-
4	120.598	120.193	114.035	86.843	59.762	45.679	46.415	53.915	45.782	45.786	120.902	-

Table 3. RPIM frequencies of the cantilever beam for various α_c (sd=3L/10, q=1).

Mode	RPIM with Gauss integration (11 nodes)					RPIM with Nodal integration (11 nodes)					FEM (100 elements)	Exact (Ferreira, 2009)
	α_c					α_c						
	1	3	5	7	9	1	3	5	7	9		
1	3.327	3.486	3.493	3.496	3.498	3.490	3.502	3.502	3.501	3.502	3.516	3.516
2	20.218	21.626	21.703	21.732	21.781	20.792	22.311	22.262	22.107	20.662	22.034	22.035
3	55.492	59.818	60.124	60.224	60.288	66.177	39.906	39.757	39.825	62.947	61.697	-
4	105.393	114.035	114.851	115.089	114.934	40.274	53.915	53.779	54.213	40.348	120.902	-

Table 4. RPIM frequencies of the cantilever beam for various q (sd=3L/10, $\alpha_c=3$).

Mode	RPIM with Gauss integration (11 nodes)					RPIM with Nodal integration (11 nodes)					FEM (100 elements)	Exact (Ferreira, 2009)
	q					q						
	0.5	0.7	0.98	1	1.3	0.5	0.7	0.98	1	1.3		
1	3.497	3.494	3.486	3.486	3.475	3.502	3.502	3.502	3.502	3.495	3.516	3.516
2	21.739	21.706	21.634	21.626	21.574	22.190	22.274	22.310	22.311	21.071	22.034	22.035
3	60.273	60.141	59.847	59.818	59.522	39.766	39.769	39.823	39.906	61.715	61.697	-
4	115.278	114.909	114.111	114.035	113.123	53.820	53.728	53.766	53.915	41.293	120.902	-

Conclusions

All methods are in excellent agreements for the deflection solutions. In the first mode of free vibration of the cantilever beam, all methods are again in good agreements. However, in the higher modes, PIM and RPIM with nodal integration and RPIM with Gauss integration give stiffer results than FEM, analytical results and PIM with Gauss integration. Increasing support domain size generally improve the results. However, when the node numbers in the support domain becomes greater than 10, the beam starts to behave more rigid. The change of α_c and q values does not significantly change the frequencies.

References

- Chandrupatla, T.R. and Belegundu, A.D. (1999), Introduction to Finite Elements in Engineering, Prentice-Hall Inc., Upper Saddle River, NJ.
- Ferreira, A. J. M. (2009), MATLAB Codes for Finite Element Analysis-Solids and Structures, Springer, Berlin.
- Gu, Y. T. and Liu, G. R. (2000), A local point interpolation method for static and dynamic analysis of thin beams, Computer Methods in Applied Mechanics and Engineering. 42, pp. 5515-5528.
- Liu, G. R. and Gu, Y. T. (2001a), A point interpolation method for two-dimensional solids. International Journal for Numerical Methods in Engineering. 50,937-951.
- Liu, G. R. and Gu, Y. T. (2001b), A local radial point interpolation method (LRPIM) for free vibration analyses of 2-D solids, Journal of Sound and Vibration. 246, pp. 29-46.
- Liu, G. R. and Gu, Y. T. (2005), An introduction to meshfree methods and their programming, Springer, Berlin.
- Liu, G. R., Zhang, G. Y., Wang Y. Y., Zhong, Z. H., Li, G. Y. and Han, X. (2007), A Nodal Integration Technique for Meshfree Radial Point Interpolation Method (NI-RPIM), Journal of Solid and Structures, vol. 44.,pp. 3845-3847.
- Wang, J. G. and Liu, G. R. (2002a), A point interpolation meshless method based on radial basis functions, Int. J. Numer. Meth. Engng. 54, pp. 1623-1648.
- Wang, J. G. and Liu, G. R. (2002b), On the optimal shape parameters of radial basis functions used for 2-D meshless methods, Comput. Methods Appl. Mech. Engrg. 191, pp. 2611-2630.